AWARD NUMBER: W81XWH-16-1-0523

TITLE: Functions of Tenascin-C and Integrin alpha9beta1 in Mediating Prostate Cancer Bone Metastasis

PRINCIPAL INVESTIGATOR: David R. Rowley, Ph.D.

CONTRACTING ORGANIZATION: Baylor College of Medicine
Houston, TX 77030

REPORT DATE: October 2017

TYPE OF REPORT: Annual

PREPARED FOR: U.S. Army Medical Research and Materiel Command
Fort Detrick, Maryland 21702-5012

REPORT DOCUMENTATION PAGE

Form Approved
OMB No. 0704-0188

1. REPORT DATE	2. REPORT TYPE	3. DATES COVERED
October 2017	Annual	30 Sept 2016 - 29 Sept 2017

4. TITLE AND SUBTITLE

Functions of Tenascin-C and Integrin alpha9beta1 in Mediating Prostate Cancer Bone Metastasis

5a. CONTRACT NUMBER

5b. GRANT NUMBER
W81XWH-16-1-0523

5c. PROGRAM ELEMENT NUMBER

6. AUTHOR(S)

David R. Rowley, Ph.D.

E-Mail: drowley@bcm.edu

5d. PROJECT NUMBER

5e. TASK NUMBER

5f. WORK UNIT NUMBER

7. PERFORMING ORGANIZATION NAME(S) AND ADDRESS(ES)

Baylor College of Medicine,
Houston, Texas 77030

8. PERFORMING ORGANIZATION REPORT NUMBER

9. SPONSORING / MONITORING AGENCY NAME(S) AND ADDRESS(ES)

U.S. Army Medical Research and Materiel Command
Fort Detrick, Maryland 21702-5012

10. SPONSOR/MONITOR'S ACRONYM(S)

11. SPONSOR/MONITOR'S REPORT NUMBER(S)

12. DISTRIBUTION / AVAILABILITY STATEMENT

Approved for Public Release; Distribution Unlimited

13. SUPPLEMENTARY NOTES

14. ABSTRACT

The purpose of this work is to dissect mechanisms responsible for interactions between integrin a9b1 and tenascin-C that are fundamental in prostate cancer metastasis to bone. Task 1 is to address the role of a9b1 using gene knockdown followed by assessment of pathway activation downstream of a9b1 and their effects on prostate cancer biology. Following some initial difficulties regarding cell viability, Substask 1 of Task 1 is nearly completed. We have generated a line of VCaP cells with inducible knockdown of alpha9 integrin. Studies are in progress to generate additional engineered cell lines for verification and we plan to also generate stable knockout cell lines using CRISPR/Cas 9 gene editing technology. Subtask 2 studies have been initiated. Substask 1 of Major Task 2 is also completed. Once engineered cell lines are validated and tested, we will initiate the remaining Subtask 3 of Major Task 1 as well as Task 2 studies. This work will advance the field by providing mechanistic data regarding the role of alpha 9 and tenascin-C in the biology of prostate cancer bone metastasis.

15. SUBJECT TERMS

Prostate cancer; bone metastasis; integrin alpha9beta1; tenascin-C

16. SECURITY CLASSIFICATION OF: U			17. LIMITATION OF ABSTRACT	18. NUMBER OF PAGES	19a. NAME OF RESPONSIBLE PERSON
a. REPORT	b. ABSTRACT	c. THIS PAGE			USAMRMC
Unclassified	Unclassified	Unclassified	Unclassified	25	19b. TELEPHONE NUMBER *(include area code)*

Table of Contents

Page

ANNUAL RESEARCH REPORT (DAMD W81XWH-16-1-0523):

1. INTRODUCTION:

This project is focused on understanding the mechanisms through which the interactions of integrin alpha9beta1 with tenascin-C act to mediate metastasis of prostate cancer cells to bone. Bone is the primary site for prostate cancer metastasis, yet mechanisms are essentially unknown and there are very limited and ineffective therapeutic approaches currently available. The overall goal of the project is to dissect and discover key mechanisms in order to develop more effective therapeutic approaches. The project uses several models developed in our laboratory that have been published.

2. KEYWORDS:

Prostate Cancer
Bone Metastasis
Integrin alpha9beta1
Tenascin-C
Bone Metastasis Models
FAK Signaling
Cell Migration

3. ACCOMPLISHMENTS:

3a. What were the major goals of the project?

The major goals of the project align with the approved SOW as stated below.

Major Task 1: Generate engineered prostate cancer cell lines with regulated knockdown of alpha 9 integrin and examine how loss of alpha 9 alters adhesion, phenotype and growth rates of PCa cells using in vitro models.

Subtask 1: Generate engineered prostate cancer cell lines with IPTG-regulated shRNA for integrin alpha 9 knockdown and control (scrambled) engineered cells. Cell lines used: VCaP and C4-2B cells. Verified VCaP in Rowley laboratory presently. C4-2B will be requested from Dr. Leland Chung and verified (MDA PCa 2bfrom ATCC may be used as an alternate).

Subtask 2: Generate efficient siRNA knockdown for FAK, c-SRC, WNK1 and SSAT. Cell lines used: VCaP and C4-2B cells. Verified VCaP in Rowley laboratory presently. C4-2B will be requested from Dr. Leland Chung and verified (MDA PCa 2bfrom ATCC may be used as an alternate).

Subtask 3: Evaluate the effects of integrin alpha 9 stable knockdown (shRNA) and FAK, c-SRC, WNK1 and SSAT (transient knockdown with siRNA) and the effects of relevant drug inhibitors on the adhesion, phenotype, and growth properties of prostate cancer cells on osteomemtic plates, 3D organoids and TBC in vitro cancer-bone interaction models.

Cell lines used: VCaP and C4-2B cells. Verified VCaP in Rowley laboratory presently. C4-2B will be requested from Dr. Leland Chung and verified (MDA PCa 2bfrom ATCC may be used as an alternate).

Major Task 2: Demonstrate how integrin α9β1 affects tumor growth and metastasis using in vivo models

Subtask 1: Complete and submit ACURO documents.

Subtask 2: Generate Xenograft models of engineered PCa cells with stable (inducible shRNA) knockdown of integrin alpha 9 using implanted 3D organoids and TBCs in nude mice and track for tumor growth**.** Cell lines used: Engineered VCaP and C4-2B cells from Aim 1. Verified VCaP in Rowley laboratory presently. C4-2B will be requested from Dr. Leland Chung and verified (MDA PCa 2bfrom ATCC may be used as an alternate). Mice used: 9 mice/set and 4 sets of experiments per 3D organoid (36 mice) and per TBC (36 mice) + 36 mice to verify with a secondary PCa cell line. = 108 mice

Subtask 3: Generate and evaluate an in vivo metastasis model using implanted 3D organoid and TBC models and engineered prostate cancer cells injected intracardially for effects of knocked down alpha 9 integrin. Cell lines used: Engineered VCaP and C4-2B cells from Aim 1. Verified VCaP in Rowley laboratory presently. C4-2B will be requested from Dr. Leland Chung and verified (MDA PCa 2bfrom ATCC may be used as an alternate).
Mice used: 9 mice/set and 4 sets of experiments per 3D organoid (36 mice) and per TBC (36 mice) + 36 mice to verify with a secondary PCa cell line. = 108 mice

3b. What was accomplished under these goals?

Major Task 1, Subtask 1: The major activities during this reporting period were to address and complete Major Task 1, Subtask 1 proposed experiments. As proposed, we completed all the studies with testing siRNAs for successful knockdown and showed that these had the same effect as the neutralizing antibody to alpha 9 integrin. To complete Major Task 1, Subtask 1, we have generated VCaP cell lines with stable and inducible knockdown of alpha 9 integrin expression (mRNA). We experienced some initial difficulties and delays with the first round of vector development and cell engineering. For this we generated six shRNA sets (two were scrambled and four were shRNA specific for alpha 9 sequences). We had several difficulties with viability and growth of infected VCaP cells. We suspect there was difficulty with the particular viral backbone undergoing recombination that led to cell viability issues. For the second round of development and screening, we used a new vector backbone (tet-inducible) and the same scrambled and specific shRNA sequences. Engineered VCaP cells were derived via puromycin selection. The second round of engineering produced VCaP lines with inducible knockdown. We are in the process of verification for tet-inducible knockdown of gene expression and knockdown efficiency. Of two positive clones, one shows tet-inducible knockdown of alpha 9 integrin expression and the other clone shows, paradoxically, a tet-inducible increase of alpha 9 expression. Although this was not intended, this clone will be useful for addressing specific mechanisms in subsequent experiments. The scrambled, control shRNA clones show no effect, as expected. We are in the process of developing additional clones of VCaP cells with tet-

inducible alpha 9 integrin knockdown, as proposed. We will next verify knockdown via examining protein levels, as proposed. As outlined in the proposal, all experiments will be conducted with VCaP cells and key results will be validated using LNCaP derivative C4-2B cells and then with MDA PCa 2b cells, as each are bone metastatic prostate cancer cell lines.

In addition to the proposed study, we plan to also produce VCaP cells that are null (knockout) for alpha 9 integrin using CRISPR/Cas9 gene editing protocols. We expect this to be completed in the next 2 months. This was not proposed in the original application; however, we feel this will be a good secondary method to assure complete knockout of alpha 9 protein. This will become important in order to verify studies with the inducible shRNA approach. We are experienced with CRISPR-Cas knockdown and have successfully engineered cells previously. We do not expect any particular difficulty in completing Subtask 1 in the next 2 months.

Major Task 1, Subtasks 2 and 3: We have made progress on Major Task 1, Subtasks 2 and 3 but have not yet completed experiments. We have acquired most of the antibodies, siRNAs, and small molecule inhibitors (drugs) as proposed for each Subtask. We are in the process and planning to fully evaluate each one for efficacy prior to use for the specific proposed experiments. We experienced a delay in conducting experiments due to the delay in engineering cell lines as discussed in Subtask1. We anticipate moving forward rather quickly once additional cell lines have been engineered. Based on our stated Milestone timeline in the approved Statement of Work (SOW) we are on pace to complete these studies as proposed. Milestone: "*Determination of how integrin alpha 9 and downstream mediators FAK, c-SRC, WNK1 and SSAT may affect prostate cancer cell adhesion, phenotype and growth on models of bone surfaces in vitro". "MONTHS 12-18".* We plan to complete Subtasks 2 & 3 in the next 6-9 months.

Major Task 2, Subtask 1**:** We have also completed Major Task 2, Subtask 1, acquiring ACURO approval for this project.

Major Task 2, Substasks 2 and 3: The proposed studies involve in vivo approaches and depend on developing the engineered cell lines generated during Major Task 1 studies. We anticipate Major Task 2 to be completed on time in year 02 and 03.

Other studies have been completed that do affect the proposed Major Task 2 studies. As part of another funded project, we have made progress on a model system that will impact the Major Task 2 studies in year 02 and 03. We have generated a chicken egg chorioallantoic membrane (CAM) model, whereby organoids of human prostate cancer / mesenchymal stem cells are placed onto the CAM of a fertilized chick egg and incubated with a bovine trabecular bone cube (TBC) coated with either control protein (BSA) or human tenascin-C. These studies show that prostate cancer cells preferentially migrated to and formed colonies on the tenascin-C coated TBC, as compared to the control TBCs. Although not proposed in the original application, use of this model will be important to Major Task 2 of the SOW, as we can use this unique in vivo model to verify the mouse in vivo studies, as originally proposed. Moreover, the CAM model will help us tease out mechanisms in a much more easily manipulated in vivo model system. We anticipate doing this in addition to the originally proposed studies in Major Task 2, as one of our additional

/ supplemental approaches to verify data. This model has now been published. See attached manuscript that is now in press (San Martin, et al., 2017, Cancer Research, In press).

3c. What opportunities for training and professional development has this project provided?

The project has been developed as a component of Ms. Linda Tran's Ph.D. Thesis project. She is supported 50% by this project. Results have been discussed with her Thesis Advisory Committee.

3d. How were results disseminated to communities of interest?

We are just completing year 01, therefore data has not been presented at a national meeting. Results have been discussed in intra-lab meetings. In addition, results have been discussed in our Bone Metastasis focus group in the Dan L Duncan Comprehensive Cancer Center at Baylor College of Medicine.

We have published the foundational information that this project was based on. Data in this manuscript was presented as preliminary data in the grant application. See attached manuscript that is now in press:

San Martin et al. Tenascin-C and integrin alpha-9 mediate prostate cancer Interactions with bone. 2017. Cancer Res. (in press). Published on line 10-24-2017, doi: 10.1158/0008-5472.CAN-17-0064.

3e. What do you plan to do during the next reporting period to accomplish the goals?

Major Task 1: We plan to continue to develop more VCaP cell lines with both tet-inducible knockdown (using shRNA) of alpha 9 integrin as well as knockout using CRISPR/Cas9 gene editing approaches, as described in section 3b. We will continue to screen engineered prostate cancer cell lines for altered signaling pathways, as proposed in the grant application. We plan to complete most of Major Task 1 by the end of the next project period. This will involve screening the engineered cell lines and determining which signaling pathway is activated by alpha 9 integrin.

Major Task 2: During year 02, we should be able to initiate the in vivo studies outlined in the grant application. We plan on completing the in vivo studies during Year 03.

4. IMPACT:

4a. What was the impact on the development of the principal discipline(s) of the project?

The published preliminary data has made an impact on the field of prostate cancer bone metastasis. This work is now in press and has been presented in part at various research

presentations at BCM. The community now knows the importance of the alpha 9 integrin and the interaction with tenascin-C. It is anticipated that this information will be of importance in generating future therapeutic and prognostic approaches.

4b. What was the impact on other disciplines?

Nothing to report yet. It is anticipated that the data gained will impact on the research conducted in other tumor systems that metastasize to bone.

4c. What was the impact on technology transfer?

Nothing to report.

4d. What was the impact on society beyond science and technology?

Nothing to report.

5. CHANGES / PROBLEMS

5a. Changes in approach and reasons for change:

There have been no changes from the original plan, tasks, or procedures to conduct the research. We have experiences somewhat of a delay in generating stable cell lines with successful and inducible knockdown of alpha 9 integrin, however we have followed the original proposed plan and now have generated these cells, as discussed in Section 3b. The only change has been to use constructs with tetracycline-induced expression of shRNA instead of IPTG-induced expression.

5b. Actual or anticipated problems or delays and actions or plans to resolve them:

The only problem encountered was generating stable cell lines with inducible shRNA knockdown of alpha 9 integrin. We did complete all the studies with testing siRNAs for successful knockdown and showed that these had the same effect as use of the neutralizing antibody to alpha 9. We believe the delay has been resolved with successful knockdown with maintained cell viability. We are also resolving this using CRISPR/Cas 9 knockout approaches as discussed in section 3b.

5c. Changes that had a significant impact on expenditures:

We have taken longer to generate stable shRNA knockdown cell lines than anticipated during year 01. This has resulted in less expenditure of funds for year 01 than we expected. We anticipate using these funds fully in year 02.

5d. Significant changes in use or care of human subjects, vertebrate animals, biohazards, and/or select agents:

We have had no changes in human cell line use, animals, biohazards or select agents.

5e. Significant changes in use or care of human subjects:

We have had no changes in use or care of human subjects.

5f. Significant changes in use or care of vertebrate animals:

We have had no significant changes in use or care of vertebrate animals.

5g. Significant changes in use of biohazards and/or select agents:

We have had no significant change in use of biohazards or select agents.

6. PRODUCTS:

6a. Publications, conference papers, and presentations:

This preliminary data that supported this project has now been published (see 6b).

6b. Journal Publications:

Preliminary work supporting this project was published in a manuscript now in press:

San Martin et al. Tenascin-C and integrin alpha-9 mediate prostate cancer Interactions with bone. 2017. Cancer Res. (in press).

6c. Books or other non-periodical, one-time publications:

Nothing to report.

6d. Other publications, conference papers, and presentations:

Nothing to report.

6e. Website(s) or other Internet site(s):

Nothing to report.

6f. Technologies or techniques:

Development of this project has led to the use of the chick chorioallantoic membrane (CAM) model to study human prostate cancer cell migration, metastasis and colony growth on trabecular bone. This model was reported in our recent publication. Although this model is not specifically proposed in this project, any data we generate with Task 2 studies (in vivo mouse studies) can be verified using the CAM bone model. This model was published in the following manuscript:

San Martin et al. Tenascin-C and integrin alpha-9 mediate prostate cancer Interactions with bone. 2017. Cancer Res. (in press).

6g. Inventions, patent applications, and/or licenses:

Nothing to report.

6f. Other Products:

Nothing to report.

7. PARTICIPANTS & OTHER COLLABORATING ORGANIZATIONS

7a. What individuals have worked on the project?

Name:	*David R. Rowley, Ph.D.*
Project Role:	*Principal Investigator*
Researcher Identifier (e.g. ORCID ID):	0000-0002-1297-8124
Nearest person month worked:	*1.2 person months*
Contribution to Project:	*Principal Investigator. Study design and supervision. Analysis of data. Writing all reports.*
Funding Support:	

Name:	*Linda Tran*
Project Role:	*Graduate Student*
Researcher Identifier (e.g. ORCID ID):	
Nearest person month worked:	*6 person months*
Contribution to Project:	*Ms. Tran conducted the experiments of Task 1. She has also been involved in animal husbandry*
Funding Support:	

Name:	*Truong D. Dang*
Project Role:	*Research Assistant / Laboratory Technician*
Researcher Identifier (e.g. ORCID ID):	
Nearest person month worked:	*6 person months*
Contribution to Project:	*Mr. Dang provided project support by culturing all cells, ordering all supplies, management of the laboratory and assisting Ms. Tran with experiments.*
Funding Support:	

7b. Has there been a change in the active other support of the PD/PI(s) or senior/key personnel since the last reporting period?

There has been a change in active support for Dr. Rowley. The following projects have been completed during the year 01 project period:

Completed: 1 R01 DK083293-01 A1 09/01/2010 to 08/31/2014 (NCE to 08/31/2016) 15% Effort 15% effort (1.8 Calendar Months on NCE)

Completed: DOD DAMD W81XWH-12-1-0197 (PC111729) 09/01/12 to 08/31/15 (NCE to 08/31/16). 10% effort (1.2 Calendar Months)

Completed: NIH 5U54 CA163124-05 (University of Michigan Subcontract to BCM) 8/1/2015 to 7/31/2016 (NCE to 7/31/17) 5% Effort (0.6 Calendar Months).

The following project has been approved and a Notice of Award has been made. Dr. Rowley is the Principal Investigator:

Funded: DOD DAMD W81XWH-17-1-0605 (PC160801) 9/1/2017 to 8/31/2020. 25% Effort (3 calendar months).

7c. What other organizations were involved as partners?

Nothing to report.

8. SPECIAL REPORTING REQUIREMENTS

8a. Collaborative Awards:

Nothing to report

8b. Quad Charts:

Nothing to report

9. APPENDICES

Publication that is currently in press (see attached Page Proofs).

San Martin et al. Tenascin-C and integrin alpha-9 mediate prostate cancer Interactions with bone. 2017. Cancer Res. (in press).

Microenvironment and Immunology

Cancer Research

Tenascin-C and Integrin α9 Mediate Interactions of Prostate Cancer with the Bone Microenvironment

Rebeca San Martin[1], Ravi Pathak[2], Antrix Jain[1], Sung Yun Jung[3], Susan G. Hilsenbeck[4], María C. Piña-Barba[5], Andrew G. Sikora[2], Kenneth J. Pienta[6], and David R. Rowley[1]

Abstract

Deposition of the extracellular matrix protein tenascin-C is part of the reactive stroma response, which has a critical role in prostate cancer progression. Here, we report that tenascin-C is expressed in the bone endosteum and is associated with formation of prostate bone metastases. Metastatic cells cultured on osteo-mimetic surfaces coated with tenascin-C exhibited enhanced adhesion and colony formation as mediated by integrin α9β1. In addition, metastatic cells preferentially migrated and colonized tenascin-C–coated trabecular bone xenografts in a novel system that employed chorioallantoic membranes of fertilized chicken eggs as host. Overall, our studies deepen knowledge about reactive stroma responses in the bone endosteum that accompany prostate cancer metastasis to trabecular bone, with potential implications to therapeutically target this process in patients. *Cancer Res; 1–14.* ©2017 AACR.

Introduction

Local prostate cancer that progresses and invades outside the gland preferentially metastasizes to bone among other tissues (1). The formation of new micrometastases and the subsequent growth of macroscopic tumors results in bone pain and potentially pathologic fracture. These metastases are primarily osteoblastic. The specific mechanisms that promote metastasis to bone are not understood; however, the role of the microenvironment in bone has been proposed as an important player in this process (1). Specifically, the mechanisms that mediate colonization of prostate cancer cells to the bone endosteum and then promote colony expansion are essentially unknown; however, alterations in adhesion have been shown to affect metastatic potential (2). The bone endosteum is a layer of cells lining the internal trabecular bone and is composed of osteoprogenitor stem cells, resting and active osteoblasts, and osteoclasts. The endosteum is the site of the osteoblastic niche in bone, which has been shown to be important for hematopoietic stem cells self-renewal (3). Importantly, this same endosteal osteoblastic niche has been shown to be the site of prostate cancer metastases, and data suggest that prostate cancer cells compete with hematopoietic stem cells for this niche (4).

Tenascin-C is a hexameric extracellular matrix protein that is evolutionary conserved in the order *Chordata* (5) and plays an essential role in the development of bone and the nervous system (6, 7). Interestingly, the expression of tenascin-C in adult, differentiated tissues at homeostasis is negligible, but its deposition is essential for wound repair (8–10). Importantly, tenascin-C is expressed at sites of new bone deposition by osteoblasts (11). During bone development, tenascin-C was found in osteogenic cells that invade cartilage during endochondral ossification and in the condensed osteogenic mesenchyme that form new bone during intramembranous ossification and around new bone spicules. These studies also showed that after bone formation, some tenascin-C remains located in the endosteum surface; however, it is not found in the mature bone matrix (12). Important to the results of the current study, elevated tenascin-C deposition is observed at sites of bone repair after fractures (13).

In prostate cancer, tenascin-C is deposited early during cancer progression and is a key hallmark of reactive stroma (14). Reactive stroma recapitulates a normal wound repair (15) and is composed of a heterogeneous population of vimentin-positive cancer-associated fibroblasts (CAF) and myofibroblasts, cells derived from tissue-resident mesenchymal stem cells (MSC) that express smooth muscle alpha actin and vimentin (VIM) upon the influence of TGFβ (16). This tenascin-C enrichment of the tumor microenvironment affects cancer cell adhesion, migration, and proliferation (17). In this context, tenascin-c also exhibits immunosuppressive functions in tumors via regulation of cytokine/chemokine expression that affects inflammation and the immune landscape (18).

The reactive stroma response in prostate cancer initiates early in the disease, during prostatic intraepithelial neoplasia (19) and is predictive of biochemical recurrence after prostatectomy (20).

[1]The Department of Molecular and Cellular Biology, Baylor College of Medicine, Houston, Texas. [2]Bobby R. Alford Department of Otolaryngology, Head and Neck Surgery, Baylor College of Medicine. Houston, Texas. [3]Department of Biochemistry and Molecular Biology, Baylor College of Medicine, Houston, Texas. [4]Biostatistics and Informatics Shared Resource Duncan Cancer Center, Houston, Texas. [5]Laboratorio de Biomateriales, Instituto de Investigaciones en Materiales, Universidad Nacional Autónoma de México, Mexico City, Mexico. [6]The James Buchanan Brady Urological Institute, Johns Hopkins University School of Medicine, Baltimore, Maryland.

Note: Supplementary data for this article are available at Cancer Research Online (http://cancerres.aacrjournals.org/).

Corresponding Author: David R. Rowley, Baylor College of Medicine and Michael E. DeBakey Veterans Association Medical Center, One Baylor Plaza, Houston, TX 77030. Phone: 713-798-6220; Fax: 713-790-1275; E-mail: drowley@bcm.edu

doi: 10.1158/0008-5472.CAN-17-0064

Persistent deposition of tenascin-C by both CAFs and myofibroblasts (21) may foster the progression of prostate cancer and initiation of metastasis via differential adhesion patterns and transient EMT induction (22).

In the case of prostate cancer, metastases preferentially target bone (23). Following Paget's "seed and soil" hypothesis (24), the colonization of a secondary site by a cancer cell that has successfully escaped the primary tumor site is dependent on a suitable environment amenable to colonization. Therefore, the possibility arises that metastatic colonization initiates a reactive response at the secondary site (25), and/or an underlying pathology at the secondary site created a "fertile soil" in which the metastatic foci preferentially colonizes. Interestingly, the microenvironment changes present in prostate cancer bone metastases, in the context of a reactive tissue phenotype, have not been characterized.

We report here a spatial association of human prostate cancer bone metastases with reactive endosteum foci high in tenascin-C deposition and dissect the role of tenascin-C in regulating adhesion and colony initiation. Selective adhesion and colony formation on bone/tenascin-C surfaces was mediated by integrin α9β1 in prostate cancer cells in novel human three-dimensional (3D) osteogenic organoids and in egg chorioallantoic membrane (CAM) metastasis models that use tenascin-C–coated, humanized, bovine trabecular bone cubes. This work extends our understanding of bone metastasis mechanisms in prostate cancer and identifies α9 integrin–tenascin-C interaction as a key mediator.

Materials and Methods

Bone metastasis tissue microarray

Human bone metastasis tissue microarrays were constructed from the rapid autopsy program at University of Michigan (Ann Arbor, MI). TMA#85 contains 63 bone metastases samples, six liver metastasis samples, three lung metastasis samples, and 12 prostate cancer samples, representing a total of 32 patients. Tissue samples from bone metastasis include 10 patients with bone marrow–associated lesions and 12 patients with trabeculae-associated metastatic foci (in triplicate). This array was analyzed via IHC for the reactive stroma markers tenascin-C, pro-collagen I, smooth muscle alpha actin, vimentin, and immune cell makers CD14 and CD68 (Supplementary Experimental Procedures, Supplementary Tables S1 and S2).

In vitro MSC-derived 3D endosteal organoid model

Human adult MSCs (Lonza) growing in T75 cell culture flasks were trypsinized using standard protocols and washed twice with 10 mL of BFS media (Supplementary Experimental Procedures) by centrifugation (400 rpm, 3 minutes). The cell pellet was resuspended in BFS media to a concentration of 4×10^5 cells/300 μL or 8×10^5 cells/300 μL. Cell culture inserts (Millipore. Millicell-CM 12 mm) were prepared as suggested by the manufacturer, and each chamber was seeded with 300 μL of the cell suspension. After overnight incubation, once MSC spheroids were formed, the BFS media in both the inner and outer chambers were substituted with complete osteogenic media (R&D CCM007 supplemented with CCM008). Osteogenic organoids were cultured for 7, 14, and 21 days, with media changes every 2 days. Control organoids were kept in BFS media for the appropriate time points, with media changes every 2 days.

For cancer coculture experiments, the media inside the insert were substituted with 300 μL of cancer cell–specific media containing 4×10^5 cells (LNCaP, VCaP, or PC3), and the media outside each insert was replaced with 600 μL of the same media, as needed. Control organoids were exposed to cancer cell media alone. After 24 hours of incubation at 37°C, 5% CO_2, the media in the outside chamber were replaced with fresh media. Coculture samples were harvested after 48 hours and processed for histology and IHC (Supplementary Experimental Procedures; Supplementary Table S3)

In vitro trabecular bone scaffold culture system

Nukbone (Biocriss S.A. de C.V.) bovine trabecular bone scaffolds, in either 200 to 500 μm particles or 0.5-cm cube were coated with human, full-length tenascin-C (Millipore cat. no. CC06) or BSA control, by immersion of the bone fragments into a 100 μg/mL solution of either protein for 7 days. Coating was confirmed by IHC (Supplementary Experimental Procedures). For *in vitro* adhesion and proliferation experiments, coated NukBone cubes were cultured with 250,000 VCaP cells in DMEM/F-12 1:1 (Invitrogen) containing 0.1% BSA, without antibiotics, using nonadhesive (CM) inserts as described before.

Prostate cancer cell lines adhesion to tenascin-C

Tenascin-C coating was done according to published protocols (26), with modifications. Using a 0.5-mm cutting template (ICN cat no 4215), we scored circles on the outside of the bottom of the cell culture wells (Osteo Assay surface, 24-well plates. cat. no. 3987 Corning or Costar nontreated, 6-well plates). In the case of the 6-well plate, 3 circles per well were inscribed. These circles were used as guides for microscopical analysis of coated surfaces. For coating, a 3 μL drop of human, full-length purified tenascin-C (Millipore cat. no. CC06) at the appropriate concentration (0, 5, 10, 25, 50, 75, and 100 μg/mL), in PBS pH 7.4, was applied in the center of each of the circles and incubated 48 hours at 37°C, until the droplets dried out. BSA at the appropriate concentrations was coated as control. Tenascin-C coating was verified as follows: coated wells were incubated for 72 hours in DMEM/F-12 1:1 (Invitrogen) containing 0.1% BSA, without antibiotics at 37°C and 5% CO_2. Plates were then fixed with 4% paraformaldehyde for 20 minutes at room temperature, and tenascin-C was detected via immunocytochemistry (AP-Vector Blue, Supplementary Experimental Procedures).

Cells (VCaP, PC3, and LNCaP) were seeded at a density of 1×10^5 cells/cm^2 in their basal media (DMEM/F-12 1:1 or RPMI) containing 0.1% BSA, without antibiotics. Cells were allowed to adhere for 3 hours at 37°C and 5% CO_2 before washing all wells three times with warm media. For imaging of adherent cells, 15 micrographs at a ×10 magnification were acquired for each of the experimental conditions, making sure to image more than 90% of the coated areas; quantification was performed with the cell counter function in the ImageJ software (27).

Neutralizing of integrin α9β1 activity

Integrin neutralization was done as according to published protocols (28). In brief, VCaP cells were incubated in DMEM/F-12 1:1 (Invitrogen) containing 0.1% BSA, supplemented with α9β1-neutralizing antibody, clone Y9A2 (BioLegend cat. no. 351603) or mouse isotype control (mouse IgG, Sigma-Aldrich cat. no. I5381), at a concentration of 10 μg/mL for 30 minutes on ice before being seeded onto the tenascin-C–coated surfaces at a density of 2.2×10^5 cells/cm^2. As described before, cells were allowed to adhere for 3 hours before washing the wells and quantification of adherent

cells. Knockdown of α9 expression via siRNA was conducted and verified as outlined in the Supplementary Experimental Procedures (Supplementary Table S4).

CAM-humanized bovine bone integrated experimental system

This system used the CAM of the chicken egg as a host for a xenograft composed of the "humanized" NukBone in combination with an organoid consisting of a mixture of VCaP cells (prostate cancer metastatic cell line) and the prostate-derived MSC hpMSC19I (16). Briefly, 8-day-old pathogen-free embryonated eggs were prepared as described previously (29) to expose the CAM. A neoprene ring was installed on top of the exposed CAM to delimit the xenograft location, and 100 μL of attachment factor (Gibco) was added in the chamber and allowed to set. The trabecular bone cube, coated with human tenascin-C[C], is placed on top. The prostate cell line–derived organoid (Supplementary Experimental Procedures) was deposited on this surface as well, about 0.5 cm away from the bone scaffold. The egg was then placed in a humidity-controlled incubator at 37°C for 6 days. Xenograft-bearing eggs were then incubated on ice for 20 minutes to anesthetize the chick. Using a syringe equipped with an 18-gauge needle, 3 mL of ice cold 4% paraformaldehyde was carefully injected through the taped window, to prevent contamination and touching the CAM/sample, to overlay the fixative over the CAM. Eggs were incubated on ice for a total of 4 hours to euthanize the chicks. The CAM was then dissected out in bulk. Tissues were placed in a 4-cm glass-bottomed cell culture dish (MatTek P35G-0-20-C) containing 5 mL of cold 4% paraformaldehyde and incubated at 4°C overnight without shaking. Tissues were then washed with three changes of PBS (5 mL each) for 5 minutes. Samples were then decalcified, paraffin embedded, and sectioned (Supplementary Experimental Procedures), taking care of embedding the xenograft with the CAM in the most proximal side of the block. For analysis of metastatic colonization of the trabecular bone fragment, 120 serial sections were acquired from each block, at a nominal thickness of 5 μm, collecting two sections per slide for a total of 60 slides. One of every eight slides were then stained with hematoxylin and eosin (H&E). Following microscopic evaluation for epithelial pockets associated with the bone, adjacent sections were analyzed by IHC studies to verify epithelial origin (pan-cytokeratin), and markers of interest (human ITGA9). Number of foci per sample were counted on the basis of the following rubric: metastatic epithelial foci is defined as (i) a collection of cuboidal cells that form clusters on the surface of the trabecular bone or (ii) a layer of cuboidal cells, in direct contact with the trabecular surface. Layers and clusters of cells, as previously described, that associated with different trabeculae and were at least 200 μm apart were counted as two separate foci. Layers and clusters of cells that associate with blood-like cells that rest atop the bone fragment were not considered as foci.

In ovo experiments followed approved protocols from the Institutional Animal Care and Use Committee.

Statistical analysis

Statistical analysis was carried out on Prism Software (GraphPad). Cell counts for adhesion experiments were analyzed using one-way ANOVA with Tukey multiple comparisons test (***, $P < 0.001$; *, $P < 0.05$). qRT-PCR analysis was analyzed by two-way ANOVA ($n = 3$; *, $P < 0.05$; **, $P < 0.01$; ***, $P < 0.001$). CAM-trabecular bone xenografts foci count data were analyzed using Student t test with Welch correction (***, $P < 0.001$).

Results

Identification of a reactive endosteum phenotype in trabeculae-associated metastatic foci of human prostate cancer

To assess a reactive phenotype in the context of bone metastasis, a human prostate cancer bone metastasis tissue array (TMA85 array, 63 metastasis samples, University of Michigan) was evaluated using dual IHC protocols as follows: tenascin-C/vimentin, smooth muscle alpha-actin/vimentin, pro-collagen I/vimentin, as well as IHC for the immune markers CD14 and CD68 (Supplementary Experimental Procedures). Image analysis revealed the bone metastasis can be classified into two distinct groups: (i) metastatic foci associated directly with the trabecular bone surface and (ii) metastatic foci associated with a reactive marrow stroma but not on the bone surface. Foci on the bone surface were associated with elevated immunoreactivity for tenascin-C in the endosteum (Fig. 1A and B), whereas smooth muscle alpha-actin staining was negligible (Fig. 1C). Of the 15 patients with trabeculae-associated metastasis, 11 showed trabecular TNC deposition in at least two of the three samples present in the array (73%). Adjacent areas immunoreactive to pro-collagen I were observed in 69% of tenascin-C–positive foci (Fig. 1B), with varying degrees of staining intensity from absent (Supplementary Fig. S1A) to high (Supplementary Fig. S1B–S1D). We subsequently termed this the reactive endosteum phenotype. In contrast, bone marrow–associated metastatic foci were negative for tenascin-C and pro-collagen deposition and showed a substantial immunoreactivity to smooth muscle alpha-actin in associated blood vessels (Fig. 1C). Elevated staining intensities of CD14 (Supplementary Fig. S2A) and CD68 macrophages (Supplementary Fig. S2B) were also observed in trabeculae-associated metastasis, when compared with marrow-associated foci.

Differentiation of MSCs in nonadhesive conditions produces 3D osteogenic organoids

To evaluate interactions of an activated endosteum and prostate cancer metastatic cell lines, a human 3D osteogenic organoid model was generated. At 7 days of osteogenic induction in nonadherent conditions, human MSCs generated spheroids that differentiated into hard, white, opalescent organoids. These organoids were apparently tethered to the sides of the cell culture insert by distinct, fibrous, and flexible tendrils (Fig. 2A). Histologic analysis of 3D organoids revealed that a central mass of cells was surrounded by a flat and compact layer of outer cells that were nearly identical to the endosteum layer associated with trabecular bone (Fig. 2A–H and E). These cells were positive for osteocalcin, alkaline phosphatase, and osteonectin (SPARC), confirming osteoblast differentiation (Fig. 2A). Interestingly, this layer was also positive for tenascin-C deposition (Fig. 2A). Immunoreactivity to smooth alpha actin, while present in control organoids, was negative in osteo-induced conditions (Supplementary Fig. S3A and S3B). Finally, control 3D organoids retain a soft, loosely aggregated structure (Supplementary Fig. S4A) with reduced viability as shown by TUNEL staining (Supplementary Fig. S4B) and IHC for cleaved caspase-3 (Supplementary Fig. S4C).

Prostate cancer cell lines preferentially adhere to tenascin-C high foci in 3D osteogenic organoids

Under coculture conditions with the 3D osteogenic organoids, the prostate bone metastatic cell line VCaP exhibited selective attachment to foci high in tenascin-C high, localized primarily on

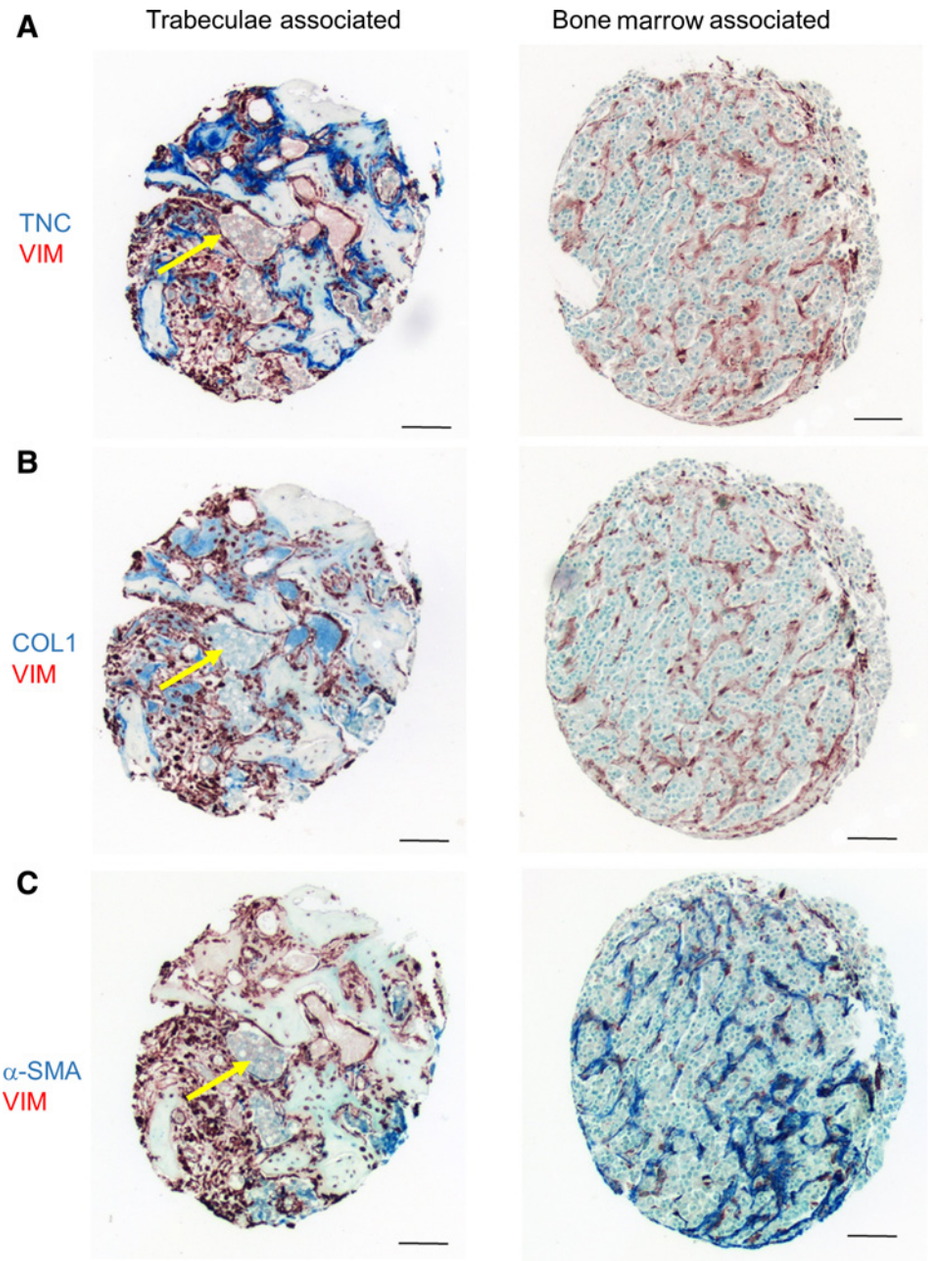

Figure 1.
Characterization of the reactive endosteum phenotype in prostate-derived bone metastasis. Bone metastasis tissue arrays were stained for reactive stroma markers. Characteristic trabeculae–associated and bone marrow metastasis samples shown. Arrows, metastatic foci. Scale bar, 100 μm. **A,** Tenascin-C (AP-Vector Blue)-vimentin (HRP-Nova Red). **B,** Pro-collagen I (AP-Vector Blue)-vimentin (HRP-Nova Red). **C,** Smooth muscle alpha actin (AP-Vector Blue)-vimentin (HRP-Nova Red).

Q7

the endosteum tendrils (Fig. 2B). Distinct branching of the endosteal tendrils around the cancer clusters was observed in some samples. In stark contrast, coculture of the 3D organoids with the metastatic line PC-3, which is osteolytic, resulted degradation of the osteogenic organoid (Supplementary Fig. S5A) creating holes in the matrix, and detachment of the endosteum tendrils from the culture vessel wall. Endosteum tendrils that remained showed the characteristic tenascin-C enrichment with clusters of cancer cells. LNCaP prostate cancer cells (derived from a lymph node metastasis) adhered to the surface of 3D osteogenic organoids and elicited a reactive degradation response of the endosteum manifested as furrows in the underlying matrix (Supplementary Fig. S5B).

Prostate cancer metastatic cells adhere to tenascin-C in a dose-dependent manner

To assess whether bone metastatic prostate cancer cell lines would adhere preferentially to tenascin-C, we used both non-treated, ~~ultralow~~ adhesion cell culture plates and Osteo Assay plates (pretreated with osteo-mimetic calcium phosphate) that were coated with increasing concentrations of human tenascin-C. A stable coating with tenascin-C was verified via immunocytochemistry (Fig. 3A and B). At 3 hours of incubation in serum-free medium, we observed a differential and concentration-dependent adhesion of VCaP cells with an optimal adhesion observed with a coating of 75 μg/mL of tenascin-C (Fig. 3C). Furthermore, adhering VCaP cells proliferated and formed 3D foci at 72 hours of

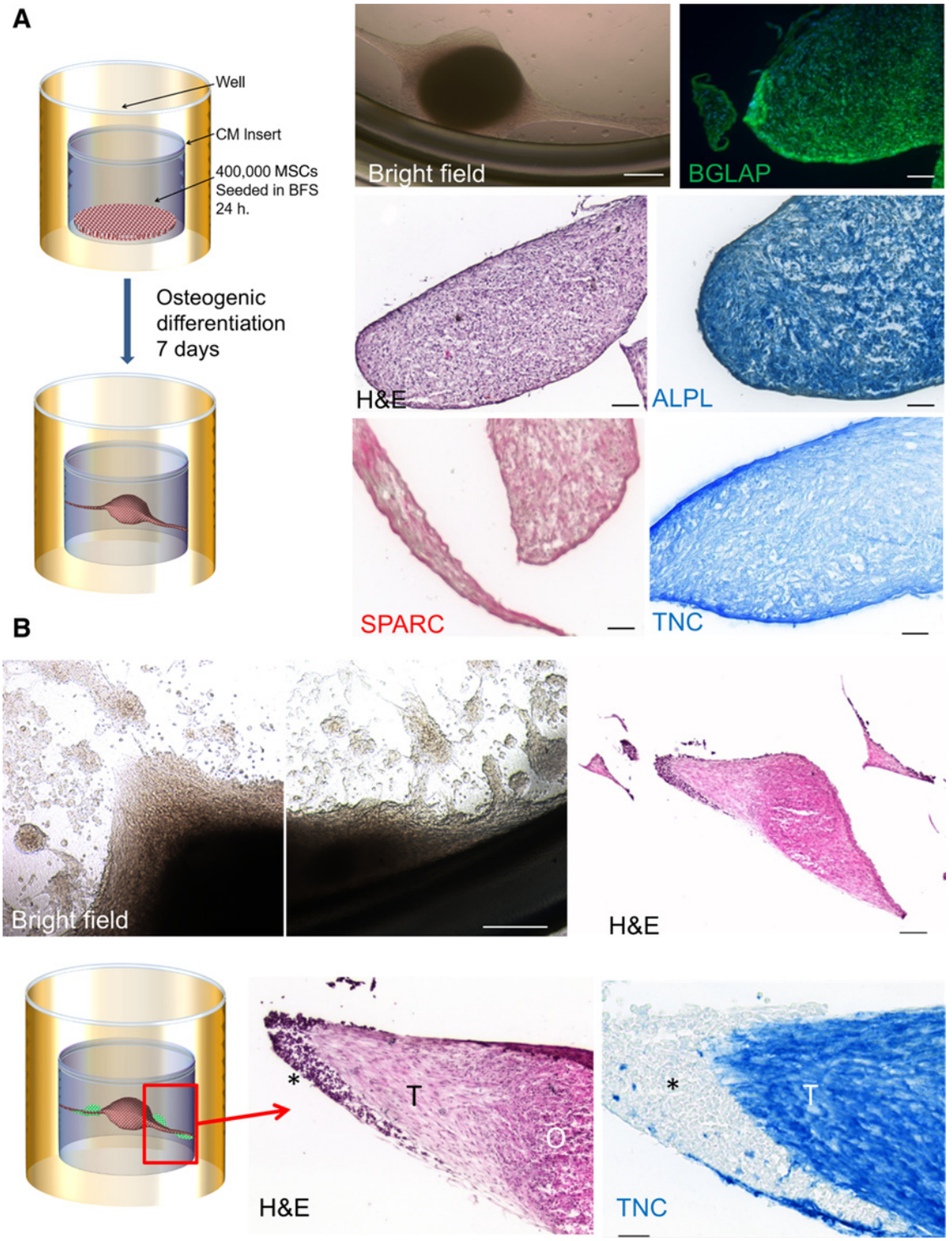

Figure 2.
MSC-derived osteogenic organoid and its interactions with the prostate cancer–derived metastatic cell line VCaP. A mesenchymal stem cell–derived osteogenic 3D spheroid model was developed to generate a fully defined, human model system where cancer and endosteum compartments are easily manipulated. **A,** Experimental protocol for organoid development. After 7 days of induction, organoids turn hard and opalescent, and develop endosteal tendrils. Brightfield image scale bar, 200 μm. The osteogenic organoid expresses osteoblast-specific markers: IF, osteocalcin (BGLAP) FITC, DAPI nuclear counterstain, H&E, IHC alkaline phosphatase (ALPL), osteonectin (SPARC), and tenascin-C (TNC). Scale bar, 100 μm. **B,** Coculture of the osteogenic organoid with the metastatic cell line VCaP. Cancer cells (*) associate at the sites of highest tenascin-C deposition, closer to the endosteal tendrils (T). Brightfield scale bar, 500 μm. H&E scale bar, 250 and 50 μm. IHC tenascin-C scale bar, 50 μm.

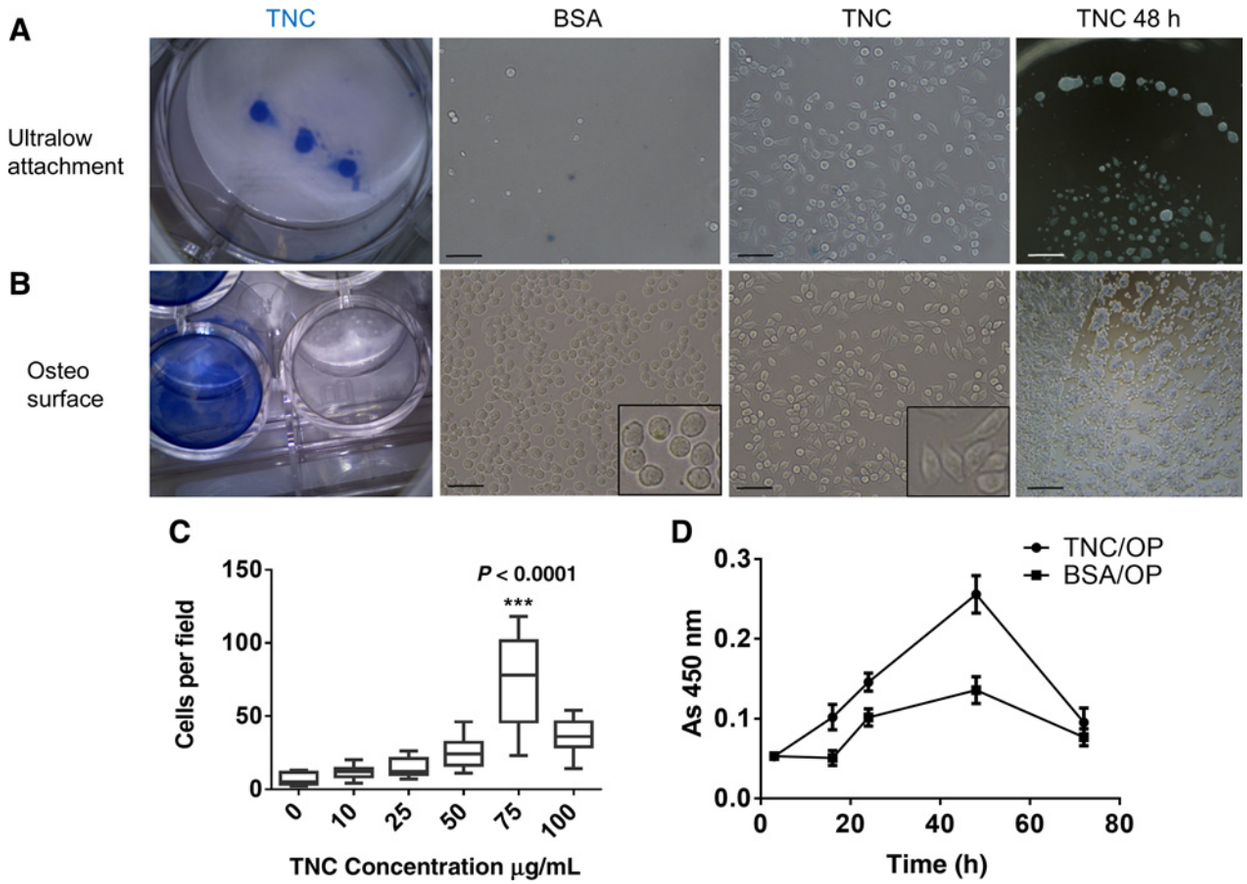

Figure 3.

VCaP adhesion and spreading in ultralow attachment and osteo-mimetic plates is enhanced by tenascin-C coating. **A,** VCaP adhesion in ultralow attachment plates. Confirmation of tenascin-C coating by immunocytochemistry (AP-Blue). VCaP attachment (3 hours) in tenascin-C, or BSA control. Note that cells flatten out and spread on tenascin-C, and they do not lift from ULA plates after washing. Scale bar, 25 μm. **B,** VCaP adhesion in osteo-mimetic plates. Confirmation of tenascin-C coating by immunocytochemistry. VCaP attachment (3 hours) to tenascin-C. Scale bar, 25 μm. VCaP culture on tenascin-C–coated surfaces form 3D foci in nonserum-containing media at 48 hours regardless of culture surface type. Scale bar, 50 μm. **C,** VCaP attachment to tenascin-C is concentration dependent. Summary of three independent experiments analyzing cell number after 24-hour culture in osteo surfaces; data, mean values ± SEM. ***, $P < 0.001$. **D**, VCaP cells attach and initiate proliferation sooner on tenascin-C–coated osteo-mimetic plates and reach higher density relative to control (BSA-coated) conditions in serum-free media. Summary of four independent experiments analyzing cell proliferation on osteo surfaces via MTT assay; data, mean values ± SEM. $P < 0.0001$.

culture in serum-free media conditions (Fig. 3A; Supplementary Fig. S6A). Interestingly, the osteoclastic cell line PC3, and the lymph node–derived cell line LNCaP did not show enhanced adhesion to tenascin-C under these conditions (Supplementary Fig. S6B and S6C, respectively), and adhere to the substrate at significantly lower levels than VCaP (Supplementary Fig. S6D).

VCaP cells grown on tenascin-C–coated Osteo Assay plates adhere readily to the surface, showing spreading as early as 3 hours after seeding (Fig. 3B) and were also able to develop 3D foci at 72 hours of culture in serum-free conditions. Cells seeded on tenascin-C–coated osteo-mimetic plates adhere and initiate proliferation upon seeding, whereas control cultures exhibit a lag time of approximately 15 to 18 hours (Fig. 3D). Thereafter, both experimental and control cells proliferate at approximately the same rate. Cultures on tenascin-C plates also reach a higher population density compared with control, with both groups seeded in serum-free media (Fig. 3D). In addition, elevated population density was confirmed with VCaP cells seeded onto human tenascin-C–coated trabecular bone scaffolds (Nuk-Bone) as compared with control conditions in both serum free and low-serum culture conditions (Supplementary Figs. S7A and S7B, respectively) as shown via MTT assay (Supplementary Fig. S7C). These trabecular bone scaffolds (Supplementary Fig. S8A) readily absorb a stable coating of tenascin-C (Supplementary Fig. S8B). Finally, VCaP cells form 3D colonies on these tenascin-C–coated scaffolds in nonserum culture conditions (Supplementary Fig. S8C).

Integrin α9β1 is essential for adhesion of prostate cancer–derived metastatic cells to tenascin-C

Owning to the rapid adhesion observed in both the low adhesion and osteo-mimetic, tenascin-C–coated cell culture conditions, we hypothesized that metastatic cell lines exhibited integrin profiles that mediated interaction with tenascin-C. Thus, a cohort of prostate cell lines (PNT1A, BPH1, LNCaP, VCaP, PC3, 22RV1, Du145, and LNCaP C4-2B) was profiled for expression of

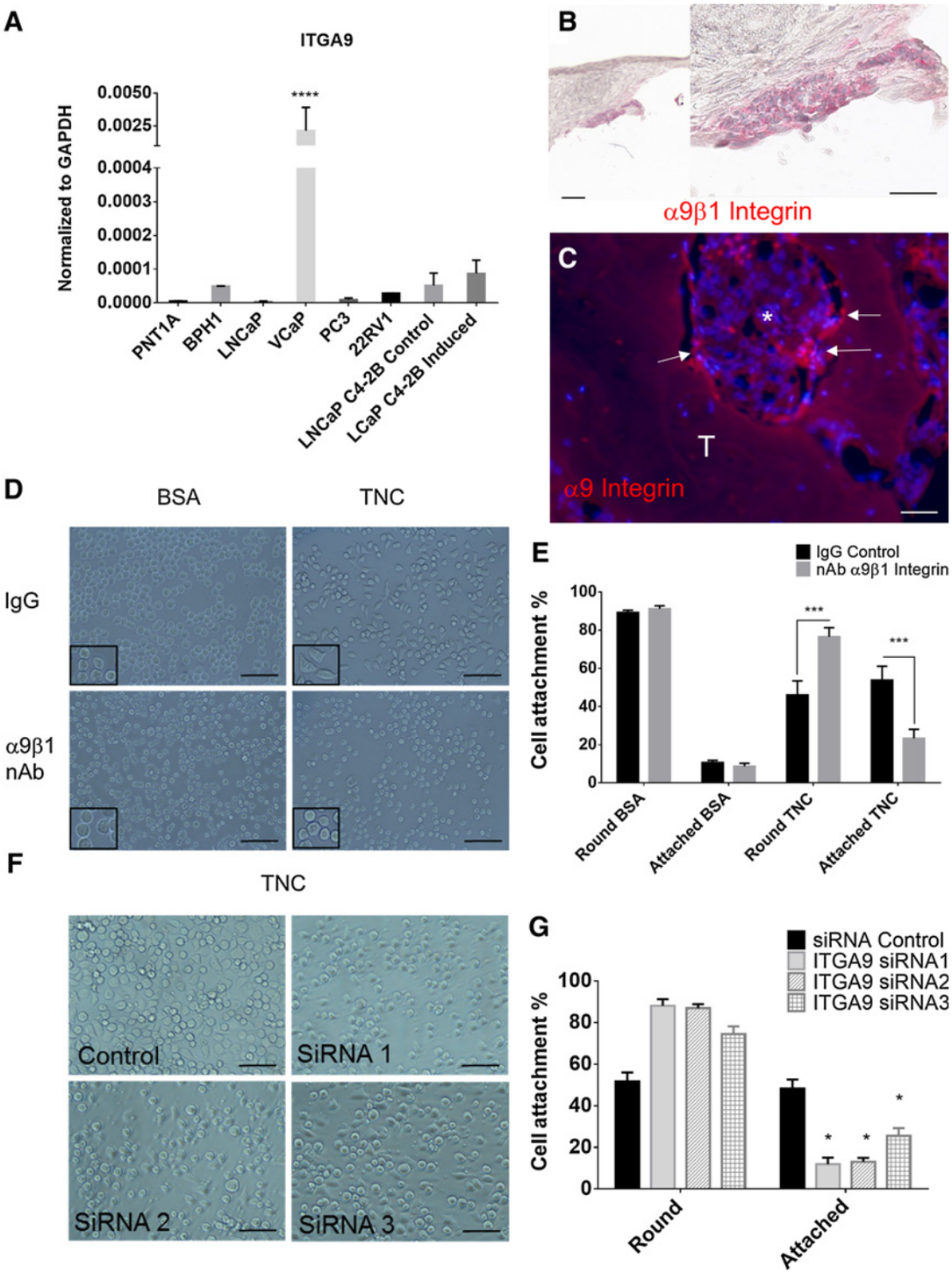

Figure 4.

VCaP adhesion to tenascin-C is mediated by α9β1 integrin. **A,** The metastatic prostate cell line VCaP expresses a significantly higher amount of integrin alpha nine when compared with other prostate cell lines. qRT-PCR data, mean values ± SEM; ****, $P < 0.0001$. **B,** Staining for the α9β1 dimer in the osteogenic organoid co culture. Scale bar 100 μm. **C,** Staining for α9 integrin (Texas Red) in the human metastasis prostate array. Image shows an adjacent section to the sample shown in Fig. 1. Metastatic foci (*) shown associated to trabecular bone (T). Arrows, ITGA9 cells. Scale bar, 100 μm. **D,** Neutralization of α9β1 via a neutralizing antibody ablates attachment to tenascin-C in VCaP. **E,** Summary of three independent α9β1 neutralization experiments on tenascin-C–coated osteo surfaces; data, mean values ± SEM. ***, $P < 0.001$. **F,** Neutralization of alpha 9 integrin via SiRNA ablates VCaP attachment to tenascin-C. **G,** Summary of three independent α9β1 knockdown-adhesion experiments on tenascin-C–coated osteo surfaces; data, mean values ± SEM.*, $P < 0.05$.

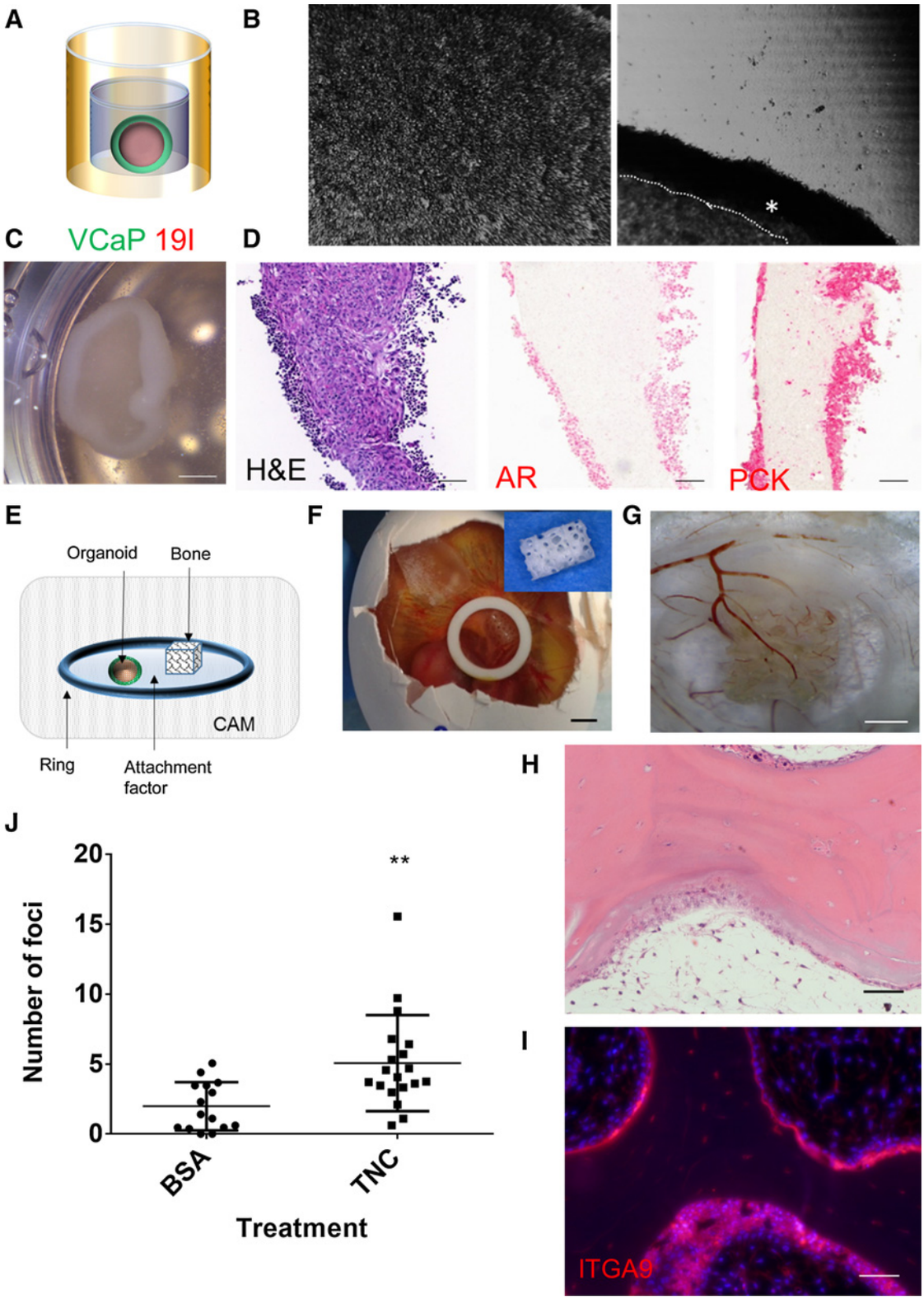
A
B
C
VCaP 19I
D
H&E
AR
PCK
E
Organoid
Bone
CAM
Ring
Attachment factor
F
G
H
I
ITGA9
J
Number of foci
20
15
10
5
0
**
BSA
TNC
Treatment

integrins known to mediate tenascin-C binding. A relatively high expression level of α9 integrin was noted in VCaP cells (Fig. 4A; Supplementary Figs. S9 and S10), which was later confirmed via IHC for the α9β1 dimer in cells associated with 3D osteogenic organoids (Fig. 4B). Furthermore, IHC analysis showed cells immunoreactive to integrin α9 in 74% of the cancer foci associated with tenascin-C in the TMA85 tissue array samples (Fig. 4C). Finally, both neutralization of the α9β1 integrin dimer via neutralizing antibodies (Fig. 4D and E) and knockdown of the α9 subunit gene expression with siRNA (Fig. 4F and G; Supplementary Fig. S11A and S11B; Supplementary Table S5; and Supplementary Experimental Procedures) ablated VCaP adhesion to tenascin-C–coated osteo-mimetic surfaces. Together, these data support the hypothesis that the α9β1 integrin plays an important role in the adhesion and colonization of prostate cancer cells in the bone metastatic niche.

Tenascin-C induces chemotaxis and colony formation of VCaP in a CAM-humanized bovine bone integrated experimental system

To model the interactions between reactive endosteum on trabecular bone and metastatic cancer cells, we developed an *in ovo* xenograft system in which a human tenascin-C–coated trabecular bovine cube was cocultured in close proximity to an organoid (Fig. 5A) comprised of bone metastatic cells (VCaP) and human prostate-derived MSCs (hpMSC 19-I) on a chicken egg CAM.

A mixture of VCAP and of hpMSC19I was cultured overnight under nonadhesive conditions to produce 3D organoids as we have reported previously (Supplementary Experimental Procedures; ref. 16). This mixture of cells starts contraction and segregation into distinct epithelial and stromal compartments as early as 3 hours after seeding (Fig. 5A, B, C). At this early time point, it is possible to detect the epithelial compartment via IHC for pan-cytokeratin and androgen receptor (Fig. 5D). These 3D organoids were placed on the CAM of the fertilized chicken egg, along with Nukbone bovine trabecular bone cubes coated with either tenascin-C or BSA as control, as described previously (Fig. 5E and F).

After 6 days of *in ovo* incubation, trabecular bone cubes recruited CAM blood vessels that infiltrate into the trabecular bone cube in a tenascin-C–independent manner (Fig. 5G). Tenascin-C–coated trabecular bone cubes show colonization of VCaP cells, identified by expression of human α9 integrin, indicating these cells migrated from the organoid toward to scaffold (Fig. 5H and I). Quantification of foci revealed that VCaP preferentially migrate to tenascin-C–coated bone fragments as compared with BSA-coated controls (Fig. 5J).

Tenascin-C elicits the production of collagen XIIa1 in metastatic prostate cells

To assess potential downstream effectors of tenascin-C–induced biology, two-dimensional RP/LC-MS analysis in VCaP cells cultured on tenascin-C–coated Osteo Assay plates was conducted (Supplementary Experimental Procedures). An increase in production of Laminin Subunit Beta 2 (LAMB2), Optineurin (OPTN), Golgi Associated, Gamma Adaptin Ear Containing, ARF Binding Protein 1 (GGA1), Phospholipase D Family Member 3 (PLD3), and Palmitoyl-Protein Thioesterase 2 (PPT2) was observed (Fig. 6A). Of relevance, a distinct increase (30-fold) of collagen12, alpha1 (COL12A1) protein was noted and subsequently confirmed in VCaP grown on 3D osteogenic organoids using IHC (Fig. 6B). Ablation of adhesion to tenascin-coated osteo plates via siRNA knockdown of integrin α9 resulted in a decrease of transcript for COL12A1 in VCaP cells cultured on tenascin-C–coated osteo-mimetic surfaces (Fig. 6C), suggesting a direct link between cell binding and this osteogenic collagen production by the epithelial cell.

Discussion

We report a reactive endosteum phenotype that accompanies trabecular bone–associated prostate cancer metastasis, characterized by elevated deposition of tenascin-C and collagen I. Although its expression is limited in adult differentiated bone, tenascin-C plays an essential role in bone repair processes, such as the formation of granulation tissue during fracture repair, in osteogenic differentiation, mineralization, and bone remodeling due to mechanical load (13, 30, 31). Furthermore, bone stromal cells and osteoblasts show increased tenascin-c expression upon *in vitro* coculture with prostate cancer–derived cell lines (32), suggesting that tenascin-c deposition could arise as a response to metastatic colonization. It has been previously suggested that prostate metastatic cells compete with hematopoietic stem cells for their niche in bone (33), a niche that has been shown to be enriched in tenascin-C during activation (34). Our studies show that bone metastatic prostate cancer cells differentially adhere, proliferate more rapidly, and form 3D colonies in tenascin-C–coated osteomimetic surfaces. Furthermore, in a 3D osteogenic organoid model, prostate cancer cells preferentially attach at sites high in tenascin-C *in vitro* and tenascin-C–coated bone fragments show enhanced metastatic colonization in an *in ovo* xenograft approach.

It is also important to note that the interaction of integrins with tenascin-C is mediated through the IDG and RGD sequences within the third fibronectin type III repeat in human tenascin-C (35). Of interest, the fibronectin type III repeat of mouse

Figure 5.
The CAM-humanized bovine bone integrated experimental system shows preferential cancer cell chemotaxis and colonization bone scaffolds enriched in tenascin-C. **A,** Graphic representation of the prostate epithelial–stroma organoid structure. Distinct hpMSC 19-I (stroma) internal compartment self-segregates from an epithelial mantle. **B,** Formation of the prostate epithelial–stroma organoid. A mixture of hpMSC 19-I and VCaP is seeded in suspension in nonadhesive conditions. Two hours after seeding, the organoid contracts and segregation of the epithelial (*) and the stromal compartments occurs (dotted line, stromal–epithelial border). Images captured with the CytoSmart live cell imaging system (Lonza). **C,** Brightfield image of the organoid at 24-hour incubation. Scale bar, 500 μm. **E,** Serial sections of the prostate organoid: H&E. IHC for androgen receptor (AR) and pan-cytokeratin (PCK) denote the epithelial compartment of the organoid. Scale bar, 100 μm. **E,** Experimental setup of the *in ovo* xenograft system. **F,** Trabecular bone scaffold *in ovo*. Inset, trabecular bone scaffold. Scale bar, 5 mm. **G,** Bulk dissection of the xenograft. Tenascin-C–coated bone xenograft after 6 days of incubation *in ovo*. The bone fragment associates with the CAM. Blood vessels infiltrate the trabecular bone xenograft. Scale bar, 2.5 mm. **H** and **I,** Serial sections of CAM-associated bone xenograft is colonized by VCaP. H&E, IF α9 integrin (Texas Red), tissue counterstained with DAPI scale bar, 100 μm. **J,** Summary of eight independent experiments (19 tenascin-C samples, 15 control), analyzing the number of VCaP foci associated with bone xenografts shows preferential recruitment to tenascin-C–coated scaffolds. ***, $P < 0.001$.

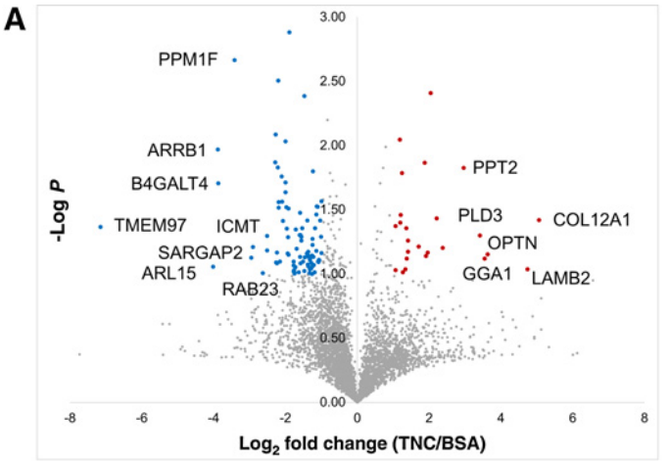

Gene ID	Gene symbol	Log_2 fold
1303	COL12A1	5.06
3913	LAMB2	4.73
10133	OPTN	3.63
26088	GGA1	3.55
23646	PLD3	3.42
9374	PPT2	2.96
51715	RAB23	-2.64
23463	ICMT	-2.90
23380	SRGAP2	-2.95
9647	PPM1F	-3.42
8702	B4GALT4	-3.87
408	ARRB1	-3.89
54622	ARL15	-4.02
27346	TMEM97	-7.15

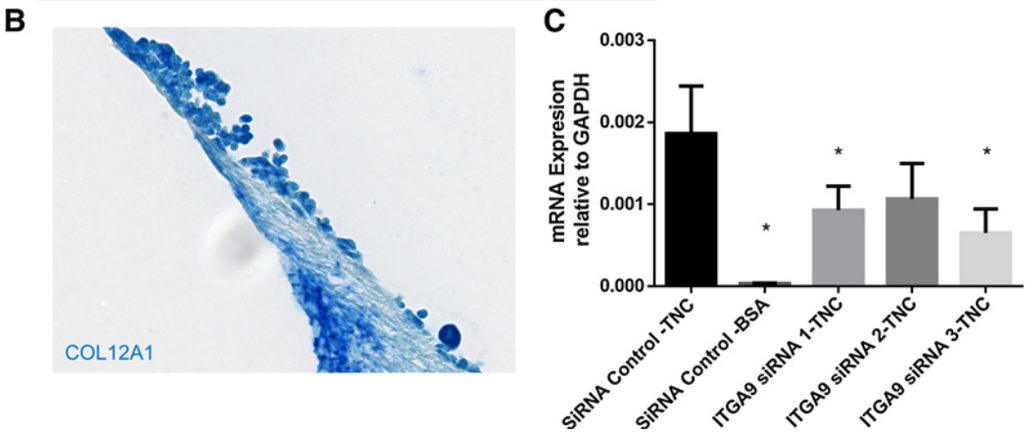

Figure 6.
Differential protein expression in VCaP cultured in tenascin-C-osteo plate. **A,** Mass spectrometry reveals enhanced expression of collagen 12A and laminin beta 2 subunit in VCaP because of culture on tenascin-C–coated osteo surfaces. **B,** VCaP that associate with the osteogenic organoid express COL12A1. IHC COL12A1, **C,** Ablation of adhesion via integrin α9 knock out decreases expression of COL12A1 in VCaP when cells are cultured on tenascin-C–coated osteo mimetic surfaces. Summary of three independent RT-PCR studies on the expression of COL12A1 upon ITGA9 knockout. *, $P < 0.05$

tenascin-C lacks the IDG and RGD sequences (35). It is possible that lack of these sequences in mouse tenascin-C may explain, in part, why transgenic mouse models of cancer rarely metastasize to bone or why injection of human cancer cells in immunocompromised mice rarely metastasize to bone. In contrast, studies where human fetal bone fragments were implanted into SCID mice showed preferential metastasis of tail vein–injected human prostate cancer cells to human bone fragments as compared with implanted mouse bone or endogenous mouse skeleton (36). In light of our results, this is not surprising, as tenascin-C expression is high in fetal human bone (11, 12).

Repetitive bone loading in normal life leads to microscopic cracks or microfractures in bone that undergoes subsequent bone repair processes. In humans, these microfractures increase with age in an exponential manner (37). Tenascin-C is overexpressed in endosteum undergoing bone repair (13). In many cancer foci, we observed elevated tenascin-C deposition in the endosteum of the trabeculae represented in the section, not just in the immediate region occupied by foci of cancer cells. It is possible that prostate cancer cells preferentially colonize the tenascin-C high reactive endosteum of bone trabeculae that are undergoing the normal process of microfracture repair as a function of aging. In this scenario, data reported here might suggest that cancer cells may not induce the reactive endosteum; rather, an existing microfracture-associated reactive endosteum is a preferential site for seeding of metastatic cells and colony initiation/formation. As tenascin-C is highly deposited in the reactive stroma of primary prostate cancers (14), it is possible that cancer cells acquire a tenascin-C addiction prior to metastasis to bone.

It is estimated that 15% of the male population will develop invasive prostate cancer in the United States (38). In most cases, resection of the primary tumor and concomitant therapies grants a 15-year recurrence-free survival. Biochemical recurrence, as refers to elevated PSA levels, is usually the first sign of prostate cancer progression, which is followed by distant metastasis in about 5% of patients. Interestingly, distant metastasis occurs 8 to 10 years after biochemical recurrence (39). The mechanisms that mediate this delay in metastatic development are not understood. Evidence suggests that tumor cells disseminate from prostate cancer in as many as 25% of patients with localized disease and that higher concentrations of these cells in blood negatively correlate with survival (40). However, it has been proposed that disseminated cancer cells become dormant in the secondary site microenvironment through several mechanisms (41, 42). We

propose that the tenascin-C–rich osteo environments used throughout our study model a normal age-related or androgen ablation–induced bone loss (43, 44) and/or subsequent incidence of subclinical microfractures. In this context, production of tenascin-C necessary for repair occurring at proximal site to a dormant foci might trigger their escape from dormancy, via differential cellular adhesion, consistent with previous findings (45).

Importantly, this study also provides evidence that metastatic prostate cancer cells interact with tenascin-C in the endosteum via the integrin α9β1 dimer (ITGA9 – ITGB1), as ablation of its activity via siRNA or neutralizing antibodies inhibits cell spreading on tenascin-C–coated osteo surfaces. Furthermore, integrin α9–positive cells are present at prostate metastatic foci enriched with tenascin-C in human samples (Fig. 5). Integrin α9β1 has been previously implicated in the induction of metastatic phenotypes in cancers where the primary tumor is also enriched in tenascin-C expression, such as breast (46–48), lung (49), and colon (50). Of key interest, α9β1 mediates the interaction between the hematopoietic stem cell and a tenascin-C–rich niche in the endosteum (34). Integrin α9β1 also plays a critical role in extravasation of neutrophils (51). Hence, the same integrin identified in the current study has been shown to mediate extravasation events and bone marrow colonization events in other normal cell types.

We also show here a significant induction in COL12A1 production by a prostate epithelial metastatic cell line (VCaP), which results from contact with tenascin-C on osteo-mimetic surfaces. Collagen XIIa (COL12A1) is a member of the fibril-associated collagens with interrupted triple helices (FACIT) family, where it contributes to the organization and mechanical properties of collagen fibrils (52). COL12A1 is present throughout mesenchymal tissues during development, but it is restricted to fascia and basement membranes in dermis, kidney, and muscle in adult organisms, a distribution that is conserved throughout vertebrate species (53). In bone development, a knockout mouse model for COL12A1 shows shorter, thinner long bones with low mechanical strength as well as decreased bone matrix deposition (54). COL12A-null osteoblasts differentiate slower with poor mineralization, showing abnormal polarization; a role in the establishment of cell–cell interactions during bone formation has been implicated (55). Given the predominantly osteoblastic nature of prostate cancer, is enticing to hypothesize that tenascin-C induced production of COL12A1 in metastatic cells would stimulate osteoblast differentiation and osteoid deposition at metastatic sites.

In conclusion, given that the reactive microenvironment response is essential for prostate cancer progression, our work on characterizing the reactive response in the bone microenvironment and what effect it has on metastasis addresses a major gap in the field. Herein, we identify tenascin-C as an extracellular component of the osteoblastic niche that fosters the colonization and growth of trabecular-associated bone metastasis. *In vitro* and *in vivo* studies established that metastatic cells bearing integrin α9β1 selectively migrate and colonize bone enriched in tenascin-C, suggesting that therapies aimed at blocking this axis will positively impact the outcome for patients with metastatic prostate cancer.

Disclosure of Potential Conflicts of Interest

No potential conflicts of interest were disclosed.

Authors' Contributions

Conception and design: ~~R.S. Martin,~~ K.J. Pienta, D.R. Rowley

Development of methodology: ~~R.S. Martin,~~ R. Pathak, A.G. Sikora, D.R. Rowley

Acquisition of data (provided animals, acquired and managed patients, provided facilities, etc.): ~~R.S. Martin,~~ R. Pathak, A. Jain, S.Y. Jung, D.R. Rowley

Analysis and interpretation of data (e.g., statistical analysis, biostatistics, computational analysis): ~~R.S. Martin,~~ S.Y. Jung, S.G. Hilsenbeck, D.R. Rowley

Writing, review, and/or revision of the manuscript: ~~R.S. Martin,~~ S.Y. Jung, S.G. Hilsenbeck, A.G. Sikora, K.J. Pienta, D.R. Rowley

Administrative, technical, or material support (i.e., reporting or organizing data, constructing databases): A. Jain, S.Y. Jung, M.C. Piña-Barba, D.R. Rowley

Study supervision: K.J. Pienta

Other (performed experiments): A. Jain

Acknowledgments

We thank Truong Dang and William Bingman III for technical assistance.

Grant Support

This work is funded by grants from CRPIT RP140616 (to D.R. Rowley), NIH NCI U01CA143055 (to D.R. Rowley and K.J. Pienta), R01CA58093 (to D.R. Rowley), the Caroline Weiss Law Endowment (to A.G. Sikora), the CPRIT Proteomics and Metabolomics Core Facility Award RP12009, CCSG P30CA125123, and the Comprehensive Cancer Center Grant NIH NCI P30CA125123 (to Baylor College of Medicine).

The costs of publication of this article were defrayed in part by the payment of page charges. This article must therefore be hereby marked *advertisement* in accordance with 18 U.S.C. Section 1734 solely to indicate this fact.

Received January 7, 2017; revised June 2, 2017; accepted September 5, 2017; published OnlineFirst xx xx, xxxx.

References

1. Jin JK, Dayyani F, Gallick GE. Steps in prostate cancer progression that lead to bone metastasis. Int J Cancer 2011;128:2545–61.
2. Lee YC, Bilen MA, Yu G, Lin SC, Huang CF, Ortiz A, et al. Inhibition of cell adhesion by a cadherin-11 antibody thwarts bone metastasis. Mol Cancer Res 2013;11:1401–11.
3. Calvi LM, Adams GB, Weibrecht KW, Weber JM, Olson DP, Knight MC, et al. Osteoblastic cells regulate the haematopoietic stem cell niche. Nature 2003;425:841–6.
4. Shiozawa Y, Pedersen EA, Havens AM, Jung Y, Mishra A, Joseph J, et al. Human prostate cancer metastases target the hematopoietic stem cell niche to establish footholds in mouse bone marrow. J Clin Invest 2011;121:1298–312.
5. Tucker RP, Drabikowski K, Hess JF, Ferralli J, Chiquet-Ehrismann R, Adams JC. Phylogenetic analysis of the tenascin gene family: evidence of origin early in the chordate lineage. BMC Evol Biol 2006;6:60.
6. Mackie EJ, Murphy LI. The role of tenascin-C and related glycoproteins in early chondrogenesis. Microsc Res Tech 1998;43:102–10.
7. Chiquet-Ehrismann R, Mackie EJ, Pearson CA, Sakakura T. Tenascin: an extracellular matrix protein involved in tissue interactions during fetal development and oncogenesis. Cell 1986;47:131–9.
8. Hakkinen L, Hildebrand HC, Berndt A, Kosmehl H, Larjava H. Immunolocalization of tenascin-C, alpha9 integrin subunit, and alphavbeta6 integrin during wound healing in human oral mucosa. J Histochem Cytochem 2000;48:985–98.
9. Okamura N, Hasegawa M, Nakoshi Y, Iino T, Sudo A, Imanaka-Yoshida K, et al. Deficiency of tenascin-C delays articular cartilage repair in mice. Osteoarthritis Cartilage 2010;18:839–48.
10. Mackie EJ, Halfter W, Liverani D. Induction of tenascin in healing wounds. J Cell Biol 1988;107:2757–67.

11. Mackie EJ, Abraham LA, Taylor SL, Tucker RP, Murphy LI. Regulation of tenascin-C expression in bone cells by transforming growth factor-beta. Bone 1998;22:301–7.
12. Mackie EJ, Thesleff I, Chiquet-Ehrismann R. Tenascin is associated with chondrogenic and osteogenic differentiation *in vivo* and promotes chondrogenesis *in vitro*. J Cell Biol 1987;105:2569–79.
13. Kilian O, Dahse R, Alt V, Zardi L, Hentschel J, Schnettler R, et al. mRNA expression and protein distribution of fibronectin splice variants and high-molecular weight tenascin-C in different phases of human fracture healing. Calcified Tissue Int 2008;83:101–11.
14. Tuxhorn JA, Ayala GE, Smith MJ, Smith VC, Dang TD, Rowley DR. Reactive stroma in human prostate cancer: induction of myofibroblast phenotype and extracellular matrix remodeling. Clin Cancer Res 2002;8:2912–23.
15. Desmouliere A, Chaponnier C, Gabbiani G. Tissue repair, contraction, and the myofibroblast. Wound Repair Regen 2005;13:7–12.
16. Kim W, Barron DA, San Martin R, Chan KS, Tran LL, Yang F, et al. RUNX1 is essential for mesenchymal stem cell proliferation and myofibroblast differentiation. Proc Natl Acad Sci U S A 2014;111:16389–94.
17. Midwood KS, Orend G. The role of tenascin-C in tissue injury and tumorigenesis. J Cell Commun Signal 2009;3:287–310.
18. Jachetti E, Caputo S, Mazzoleni S, Brambillasca CS, Parigi SM, Grioni M, et al. Tenascin-C Protects Cancer Stem-like Cells from Immune Surveillance by Arresting T-cell Activation. Cancer Res 2015;75:2095–108.
19. Tuxhorn JA, Ayala GE, Rowley DR. Reactive stroma in prostate cancer progression. J Urol 2001;166:2472–83.
20. Ayala GE, Tuxhorn JA, Wheeler TM, Frolov A, Scardino PT, Ohori M, et al. Reactive stroma as a predictor of biochemical free recurrence in prostate cancer. Clin Cancer Res 2003;9:4792–801.
21. Schauer IG, Ressler SJ, Tuxhorn JA, Dang TD, Rowley DR. Elevated epithelial expression of interleukin-8 correlates with myofibroblast reactive stroma in benign prostatic hyperplasia. Urology 2008;72:205–13.
22. Huang W, Chiquet-Ehrismann R, Moyano JV, Garcia-Pardo A, Orend G. Interference of tenascin-C with syndecan-4 binding to fibronectin blocks cell adhesion and stimulates tumor cell proliferation. Cancer Res 2001;61:8586–94.
23. Bubendorf L, Schopfer A, Wagner U, Sauter G, Moch H, Willi N, et al. Metastatic patterns of prostate cancer: an autopsy study of 1,589 patients. Hum Pathol 2000;31:578–83.
24. Paget S. The distribution of secondary growths in cancer of the breast. 1889. Cancer Metast Rev 1989;8:98–101.
25. Bonfil RD, Chinni S, Fridman R, Kim HR, Cher ML. Proteases, growth factors, chemokines, and the microenvironment in prostate cancer bone metastasis. Urologic Oncol 2007;25:407–11.
26. Probstmeier R, Pesheva P. Tenascin-C inhibits beta1 integrin-dependent cell adhesion and neurite outgrowth on fibronectin by a disialoganglioside-mediated signaling mechanism. Glycobiology 1999;9:101–14.
27. Schneider CA, Rasband WS, Eliceiri KW. NIH Image to ImageJ: 25 years of image analysis. Nat Methods 2012;9:671–5.
28. Taooka Y, Chen J, Yednock T, Sheppard D. The integrin alpha9beta1 mediates adhesion to activated endothelial cells and transendothelial neutrophil migration through interaction with vascular cell adhesion molecule-1. J Cell Biol 1999;145:413–20.
29. Li M, Pathak RR, Lopez-Rivera E, Friedman SL, Aguirre-Ghiso JA, Sikora AG. The *in ovo* chick chorioallantoic membrane (CAM) assay as an efficient xenograft model of hepatocellular carcinoma. J Vis Exp 2015;
30. Morgan JM, Wong A, Yellowley CE, Genetos DC. Regulation of tenascin expression in bone. J Cell Biochem 2011;112:3354–63.
31. Webb CM, Zaman G, Mosley JR, Tucker RP, Lanyon LE, Mackie EJ. Expression of tenascin-C in bones responding to mechanical load. J Bone Miner Res 1997;12:52–8.
32. Sung SY, Hsieh CL, Law A, Zhau HE, Pathak S, Multani AS, et al. Coevolution of prostate cancer and bone stroma in three-dimensional coculture: implications for cancer growth and metastasis. Cancer Res 2008;68:9996–10003.
33. Yu C, Shiozawa Y, Taichman RS, McCauley LK, Pienta K, Keller E. Prostate cancer and parasitism of the bone hematopoietic stem cell niche. Crit Rev Eukaryot Gene Expr 2012;22:131–48.
34. Nakamura-Ishizu A, Okuno Y, Omatsu Y, Okabe K, Morimoto J, Uede T, et al. Extracellular matrix protein tenascin-C is required in the bone marrow microenvironment primed for hematopoietic regeneration. Blood 2012;119:5429–37.
35. Adams JC, Chiquet-Ehrismann R, Tucker RP. The evolution of tenascins and fibronectin. Cell Adh Migr 2015;9:22–33.
36. Nemeth JA, Harb JF, Barroso U Jr, He Z, Grignon DJ, Cher ML. Severe combined immunodeficient-hu model of human prostate cancer metastasis to human bone. Cancer Res 1999;59:1987–93.
37. Schaffler MB, Choi K, Milgrom C. Aging and matrix microdamage accumulation in human compact bone. Bone 1995;17:521–25.
38. Siegel RL, Miller KD, Jemal A. Cancer statistics, 2015. CA Cancer J Clin 2015;65:5–29.
39. Boorjian SA, Thompson RH, Tollefson MK, Rangel LJ, Bergstralh EJ, Blute ML, et al. Long-term risk of clinical progression after biochemical recurrence following radical prostatectomy: the impact of time from surgery to recurrence. Eur Urol 2011;59:893–9.
40. Danila DC, Heller G, Gignac GA, Gonzalez-Espinoza R, Anand A, Tanaka E, et al. Circulating tumor cell number and prognosis in progressive castration-resistant prostate cancer. Clin Cancer Res 2007;13:7053–8.
41. van der Toom EE, Verdone JE, Pienta KJ. Disseminated tumor cells and dormancy in prostate cancer metastasis. Curr Opin Biotechnol 2016;40:9–15.
42. Shiozawa Y, Berry JE, Eber MR, Jung Y, Yumoto K, Cackowski FC, et al. The marrow niche controls the cancer stem cell phenotype of disseminated prostate cancer. Oncotarget 2016;7:41217–32.
43. Mittan D, Lee S, Miller E, Perez RC, Basler JW, Bruder JM. Bone loss following hypogonadism in men with prostate cancer treated with GnRH analogs. J Clin Endocrinol Metab 2002;87:3656–61.
44. Greenspan SL, Coates P, Sereika SM, Nelson JB, Trump DL, Resnick NM. Bone loss after initiation of androgen deprivation therapy in patients with prostate cancer. J Clin Endocrinol Metab 2005;90:6410–7.
45. Ruppender N, Larson S, Lakely B, Kollath L, Brown L, Coleman I, et al. Cellular Adhesion Promotes Prostate Cancer Cells Escape from Dormancy. PLoS One 2015;10:e0130565.
46. Ota D, Kanayama M, Matsui Y, Ito K, Maeda N, Kutomi G, et al. Tumor-alpha9beta1 integrin-mediated signaling induces breast cancer growth and lymphatic metastasis via the recruitment of cancer-associated fibroblasts. J Mol Med 2014;92:1271–81.
47. Ioachim E, Charchanti A, Briasoulis E, Karavasilis V, Tsanou H, Arvanitis DL, et al. Immunohistochemical expression of extracellular matrix components tenascin, fibronectin, collagen type IV and laminin in breast cancer: their prognostic value and role in tumour invasion and progression. Eur J Cancer 2002;38:2362–70.
48. Oskarsson T, Acharyya S, Zhang XH, Vanharanta S, Tavazoie SF, Morris PG, et al. Breast cancer cells produce tenascin C as a metastatic niche component to colonize the lungs. Nat Med 2011;17:867–74.
49. Sun X, Fa P, Cui Z, Xia Y, Sun L, Li Z, et al. The EDA-containing cellular fibronectin induces epithelial-mesenchymal transition in lung cancer cells through integrin alpha9beta1-mediated activation of PI3-K/AKT and Erk1/2. Carcinogenesis 2014;35:184–91.
50. Gulubova M, Vlaykova T. Immunohistochemical assessment of fibronectin and tenascin and their integrin receptors alpha5beta1 and alpha9beta1 in gastric and colorectal cancers with lymph node and liver metastases. Acta Histochem 2006;108:25–35.
51. Mambole A, Bigot S, Baruch D, Lesavre P, Halbwachs-Mecarelli L. Human neutrophil integrin alpha9beta1: up-regulation by cell activation and synergy with beta2 integrins during adhesion to endothelium under flow. J Leukoc Biol 2010;88:321–7.
52. Chiquet M, Birk DE, Bonnemann CG, Koch M. Collagen XII: Protecting bone and muscle integrity by organizing collagen fibrils. Int J Biochem Cell Biol 2014;53:51–4.
53. Bader HL, Keene DR, Charvet B, Veit G, Driever W, Koch M, et al. Zebrafish collagen XII is present in embryonic connective tissue sheaths (fascia) and basement membranes. Matrix Biol 2009;28:32–43.
54. Izu Y, Ezura Y, Koch M, Birk DE, Noda M. Collagens VI and XII form complexes mediating osteoblast interactions during osteogenesis. Cell Tissue Res 2016;364:623–35.
55. Izu Y, Sun M, Zwolanek D, Veit G, Williams V, Cha B, et al. Type XII collagen regulates osteoblast polarity and communication during bone formation. J Cell Biol 2011;193:1115–30.

AUTHOR QUERIES

AUTHOR PLEASE ANSWER ALL QUERIES

Q1: Page: 1: AU: Per journal style, genes, alleles, loci, and oncogenes are italicized; proteins are roman. Please check throughout to see that the words are styled correctly. AACR journals have developed explicit instructions about reporting results from experiments involving the use of animal models as well as the use of approved gene and protein nomenclature at their first mention in the manuscript. Please review the instructions at http://aacrjournals.org/content/authors/editorial-policies#genenomen to ensure that your article is in compliance. If your article is not in compliance, please make the appropriate changes in your proof.

Q2: Page: 1: Author: Please verify the drug names and their dosages used in the article.

Q3: Page: 1: Author: Please verify the edits made in the right running head for correctness.

Q4: Page: 1: Author: Please verify the affiliations and their corresponding author links.

Q5: Page: 1: Author: Please verify the corresponding author's details.

Q6: Page: 1: Author: Please verify the edits made in the sentence "Here, we report . . .. bone metastases" for correctness.

Q7: Page: 4: Author: Please confirm quality/labeling of all images included within this article. Thank you.

Q8: Page: 11: AU:/PE: The conflict-of-interest disclosure statement that appears in the proof incorporates the information from forms completed and signed off on by each individual author. No factual changes can be made to disclosure information at the proof stage. However, typographical errors or misspelling of author names should be noted on the proof and will be corrected before publication. Please note if any such errors need to be corrected. Is the disclosure statement correct?

Q9: Page: 11: Author: The contribution(s) of each author are listed in the proof under the heading "Authors' Contributions." These contributions are derived from forms completed and signed off on by each individual author. As the corresponding author, you are permitted to make changes to your own contributions. However, because all authors submit their contributions individually, you are not permitted to make changes in the contributions listed for any other authors. If you feel strongly that an error is being made, then you may ask the author or authors in question to contact us about making the changes. Please note, however, that the manuscript would be held from further processing until this issue is resolved.

Q10: Page: 11: Author: Please verify the headings Acknowledgments and Grant Support and their content for correctness.

Q11: Page: 12: Author: Please provide volume and page range for ref. 29.

AU: Below is a summary of the name segmentation for the authors according to our records. The First Name and the Surname data will be provided to PubMed when the article is indexed for searching. Please check each name carefully and verify that the First Name and Surname are correct. If a name is not segmented correctly, please write the correct First Name and Surname on this page and return it with your proofs. If no changes are made to this list, we will assume that the names are segmented correctly, and the names will be indexed as is by PubMed and other indexing services.

First Name	**Surname**
~~Rebeca San~~	~~Martin~~
Ravi	Pathak
Antrix	Jain
Sung Yun	Jung
Susan G.	Hilsenbeck
María C.	Piña-Barba
Andrew G.	Sikora
Kenneth J.	Pienta
David R.	Rowley